MLF Experimental Report	提出日 Date of Report August 9, 2010
課題番号 Project No. 2009B0017 実験課題名 Title of experiment Heterogeneous Deformation Behavior of Ti Alloys Studied by In-Situ Neutron Diffraction During Tensile Deformation 実験責任者名 Name of principal investigator Satoshi MOROOKA 所属 Affiliation Yokohama National University	装置責任者 Name of responsible person Kazuya AIZAWA 装置名 Name of Instrument/（BL No.） Engineering Diffractometer (BL-19) 実施日 Date of Experiment May 29, 2010 – May 31, 2010

試料、実験方法、利用の結果得られた主なデータ、考察、結論等を、記述して下さい。（適宜、図表添付のこと）
Please report your samples, experimental method and results, discussion and conclusions. Please add figures and tables for better explanation.

1. 試料 Name of sample(s) and chemical formula, or compositions including physical form.

A commercially pure titanium (CP-Ti) and a Ti-Fe-O-(N) based alloy were used in this investigation. The Ti-Fe-O alloy, which is a near a-type titanium alloy, has been proposed for a new high-strength titanium alloy. The alloy derives its strength from solid solution hardening by interstitial elements such as oxygen and nitrogen. The supersaturation of iron leads to retention of β phase, which is effective to refine a matrix structure. Their chemical compositions and scattering length density are tabulated in **Table 1**. The CP-Ti and the Ti-Fe-O alloy were prepared by hot-rolling at 1123 K to plates with 30 mm in thickness after annealing at 1023K for 3.6 ks. And then, the Ti-Fe-O alloy was prepared by groove-rolling at 1273K (HGR).

Table1 Chemical compositions and scattering length density of Ti alloys used in this investigation (mass%).

Alloy	Fe	O	N	C	Si	Ni	Sn	Al	Cr	H	Ti
CP-Ti mass%	0.2	0.15	0.5	-	-	-	-	-	-	0.015	Bal.
Scattering length density				-5.269e+10							
Ti-Fe-O mass%	0.994	0.386	0.003	0.003	0.013	0.014	0.002	0.006	0.010	0.0005	Bal.
Scattering length density				-5.356e+10							

2. 実験方法及び結果（実験がうまくいかなかった場合、その理由を記述してください。）
Experimental method and results. If you failed to conduct experiment as planned, please describe reasons.

[Experimental method] Cylindrical tensile specimens with 3 mm in diameter and 45 mm in gauge length were machined. Time-of-flight (TOF) in situ neutron diffraction measurements were performed using TAKUMI at J-PARC. A tension tester was made in such a way that the central position of a specimen does not move when a specimen is elongated. The geometrical arrangement for diffraction measurement in the axial and the transverse directions of the specimen is illustrated in **Figure 1**. The sampling volume for neutron diffraction is wide range at the parallel position of the tensile specimen, so that bulky averaged information is obtained.

2. 実験方法及び結果（つづき） Experimental method and results (continued)

[Experimental result] Examples of diffraction profiles obtained for CP-Ti and Ti-Fe-O-HGR alloy are presented in **Figure 2**. The hk.l peak intensities in the axial and transverse directions are different, indicating strong texture and, the background in the transverse direction was not linear due to the incoherent scattering. As seen in (b), (10.1) peak was split off two peaks. These peaks were α- titanium phase and oxygen concentrated α- titanium phase (Ti_xO). **Figure 3** shows the change in α-titanium (10.1) diffraction profile with the applied stress in CP-Ti. It is found that the peak moves towards the wider spacing side in the axial direction while the narrower in the transverse, with loading. When unloaded, the peaks move back towards the opposite side. Such peak shifts with loading and unloading were examined for the other diffraction peaks of (10.0), (00.2), (10.2), (11.0), (10.3), (11.2) and (20.1) for the three titanium alloys.

Figure 4a and b shows the lattice strain determined from shifts of α-Ti (10.0), (00.2), (10.1) and Ti_xO(10.1) diffraction peaks, $\varepsilon_{10.0}$, $\varepsilon_{00.2}$, $\varepsilon_{10.1}$ and ε_{TixO} as a function of the applied stress for the CP-Ti and the Ti-Fe-O-HGR alloy. As is observed in **Figure 4a** for the CP-Ti, $\varepsilon_{10.0}$, $\varepsilon_{00.2}$ and $\varepsilon_{10.1}$ in the axial direction increase linearly with increasing of the applied stress in the beginning of deformation indicating elastic regime. From the different slopes, it is found so called the diffraction. Young modulus $E_{hk.l}$ for [10.0] and [10.1] is slightly larger than that for [00.2]. The obtained values of $E_{10.0}$, $E_{00.2}$ and $E_{10.1}$ are approximately 128 GPa, 113 GPa and 120 GPa, respectively. After yielding (see YS in the figure), (00.2) lattice strain increases while (10.0) and (10.1) decreases slightly or not changes with increasing of the applied stress. This implies that the (10.0) and (10.1) family grains are plastically softer than (00.2) grains, resulting in stress partitioning that is called intergranular stresses. Then, at around the applied stress of 110MPa, (10.0) and (10.1) lattice strain increases again and the increasing rate of (00.2) lattice strain becomes smaller, indicating that the onset of plastic flow in (00.2) family grains. This region must correspond to “grain to grain yielding” being associated with Schmid factors and work hardening characters of individual grains. Since the stress partitioning among (10.0), (00.2) and (10.1) family grains estimated from the observed lattice strain change continues to a higher stress, the residual strains are observed after unloading in **Figure 4c**. The residual (00.2) strain is tensile while the (10.0) and (10.1) one is compressive. Such intergranular stresses are generated due to heterogeneous plastic flow among various [*hk.l*] family grains, where [00.2] family grains belong to harder grains while [10.0] and [10.1] softer ones.

As seen in **Figure 4b**, both α-Ti (10.0) and (10.1) and Ti_xO(10.1) strains in the axial direction increase with increasing of the applied stress linearly in the beginning. After the onset of plastic flow, i.e., yielding, lattice strain in α-Ti (10.0) and (10.1) hardly changes or slightly decreases with increasing of the applied stress. On the other hand, lattice plane strain in Ti_xO(10.1) increases greatly with an increasing in the applied stress after the yielding.

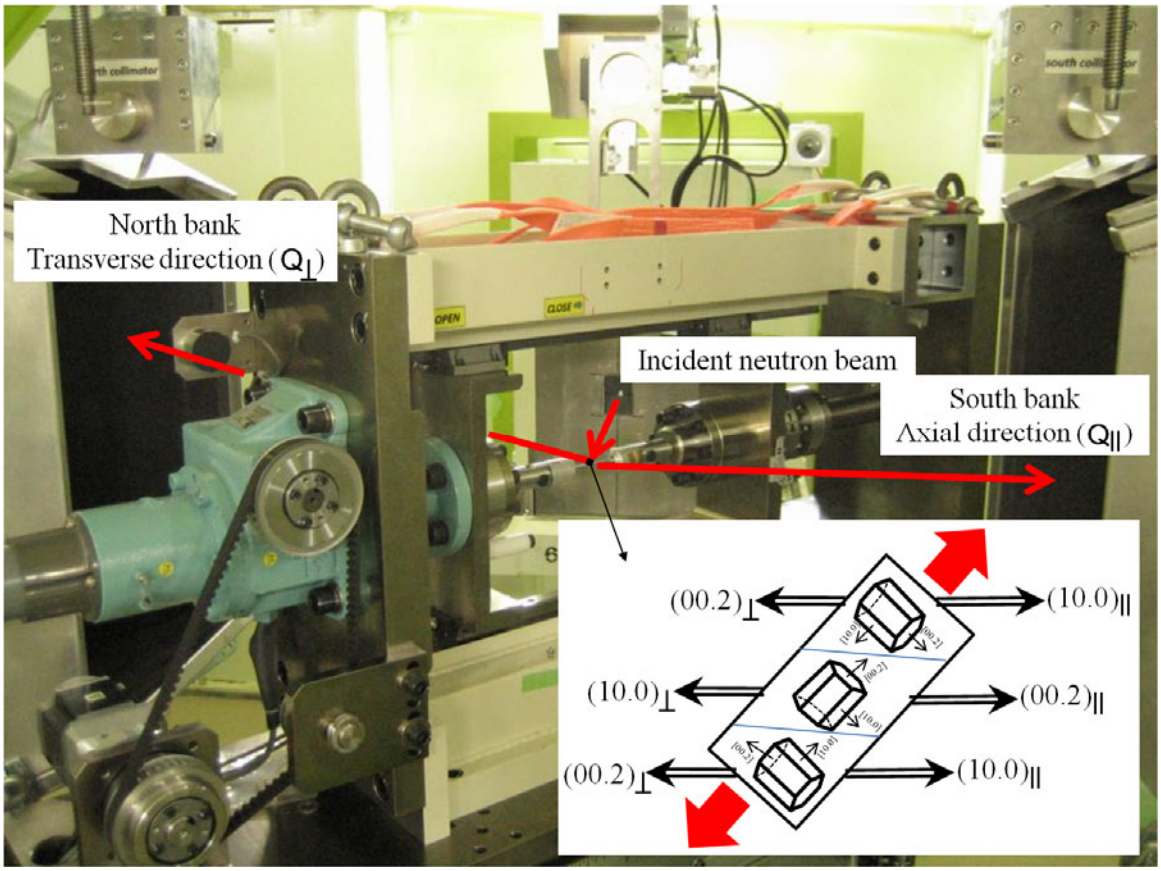

Figure 1 Schematic illustration of the diffraction geometry adopted on TAKUMI and the principle of collecting the *in situ* neutron diffraction.

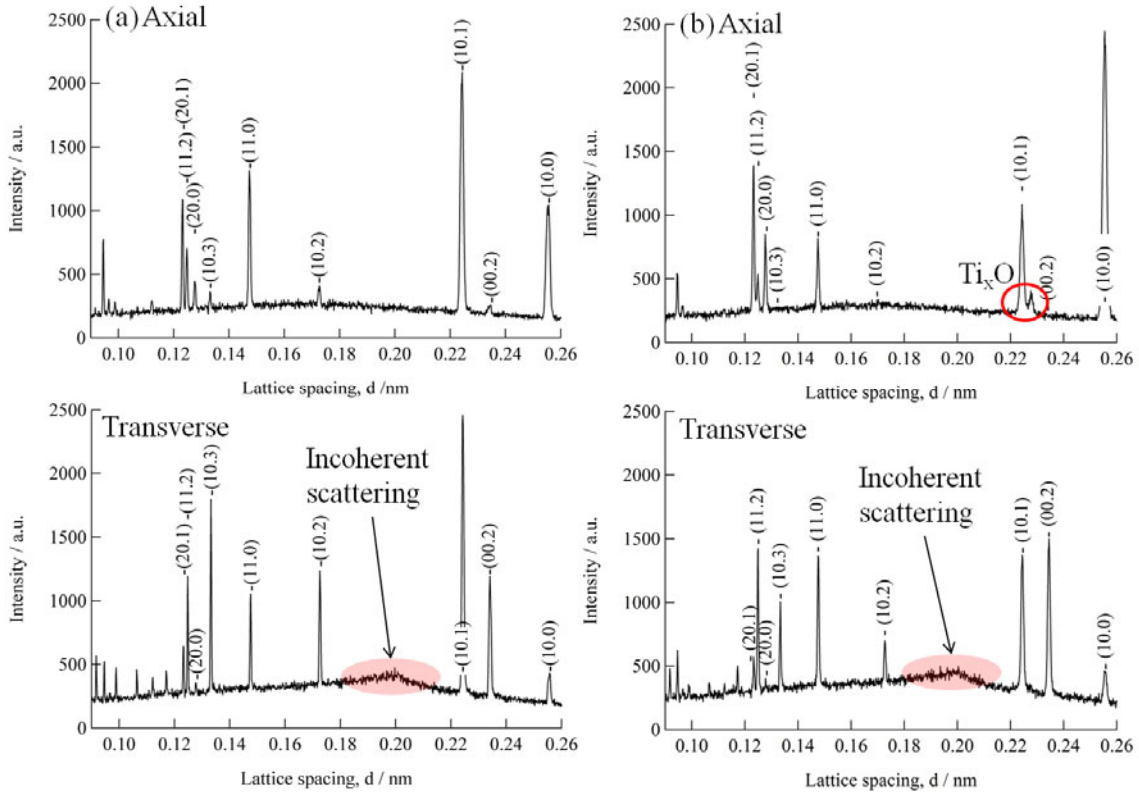

Figure 2 Diffraction profiles obtained during tensile loading in the CP-Ti (a) and the Ti-Fe-O-HGR alloy (b).

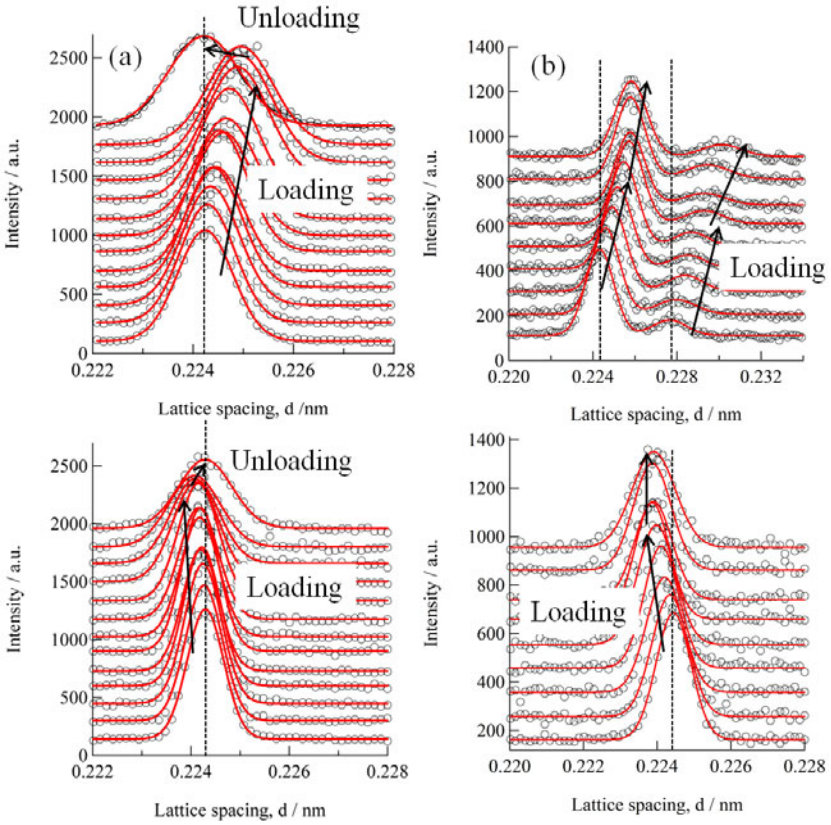

Figure 3 Changes in a titanium (10.1) diffraction profiles with tensile loading in the CP-Ti (a) and Ti-Fe-O-HGR alloy (b).

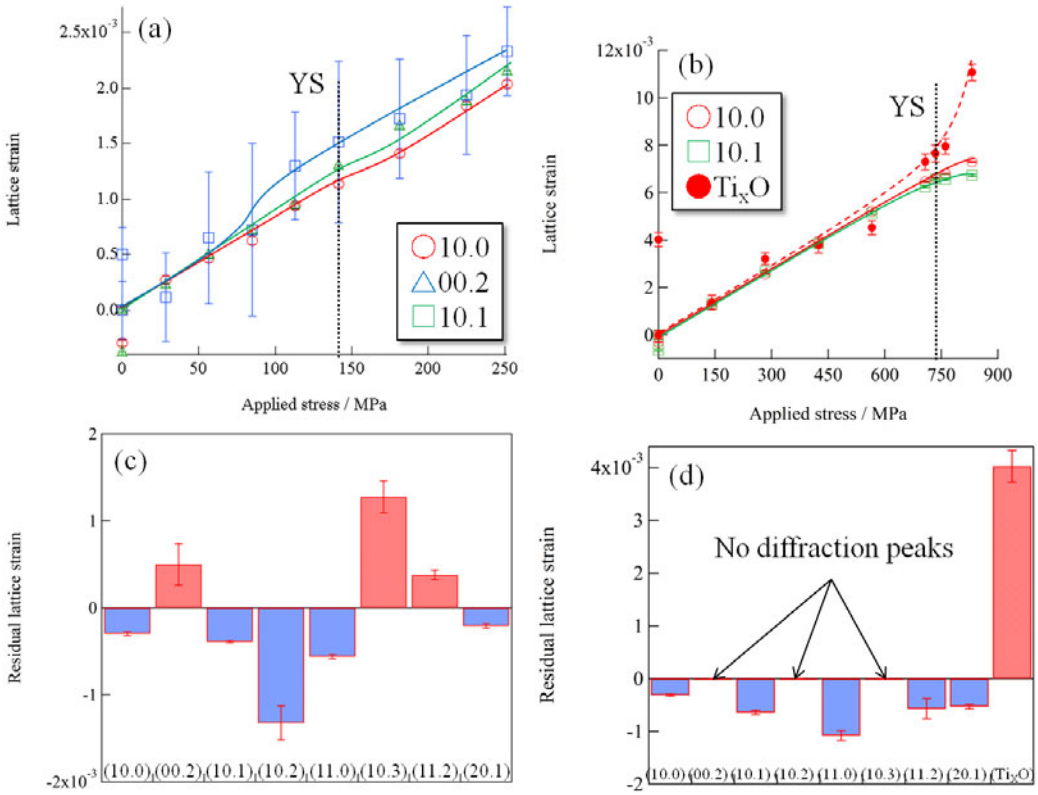

Figure 4 (a and b) (10.0), (00.2) and (10.1) lattice strains as a function of the applied stress in the axial direction for CP-Ti and Ti-Fe-O-HGR alloy. (c and d) Residual lattice strains obtained after tensile deformation for the two titanium, CP-Ti and Ti-Fe-O-HGR alloy.